This section was installed on 5/13/14 so do no edit here!

6.5. The Proximity Effect for Parallel Round Wires 1
(a) The surface charge density and its moments 1
(b) The Proximity Effect 4
(c) Plots of the Proximity Effect 6
(d) The relationship between $J_z(a,\theta)$ and $n(\theta)$: the div E = 0 approach 10
(e) The relationship between $J_z(a,\theta)$ and $n(\theta)$ as a limit of (6.5.14) 12
(f) The Proximity Effect At Low Frequencies 13

6.5. The Proximity Effect for Parallel Round Wires

This effect is discussed qualitatively in Appendix P in terms of eddy currents, and we quote the following Figure P.13,

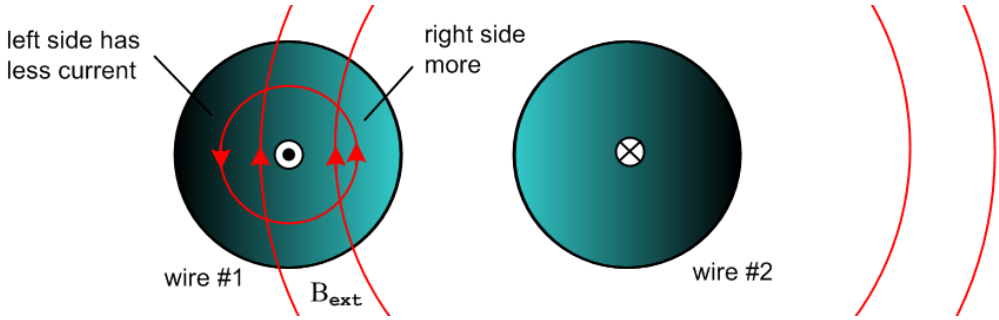

Fig 6.6

The effect is that for $\omega>0$ the current density J_z is not uniform in the conductor cross sections but is larger on the side of each conductor which faces the other conductor.

In this section we shall compute J_z over the wire cross section and perimeter to get a quantitative result.

(a) The surface charge density and its moments

On either of the conductors shown above, there is some surface charge density $n(\theta)$ which has moments called N_m and η_m in Appendix D. Using the electro-quasi-static model for a transmission line, one can analyze the transmission line as if it were an electrostatics capacitor problem. The two cylinders form a capacitor (per unit length). If one assumes a potential V between the conductors, one can solve the Laplace equation to get the potential φ in the dielectric between the conductors, which φ will be constant on the surface of either conductor. From this one may compute the electric field in the dielectric, and from the electric field just above the conductors surfaces one can compute $n(\theta)$. This calculation is carried out in our (downloadable) document *Bipolar Coordinates and the Two-Cylinder Capacitor* from which we quote results below. Each cylinder of the transmission line is characterized by a certain value of B as shown in Fig 6.2. In *Bipolar* B is called ξ which is one of the bipolar coordinates (ξ,u). The angle θ is

measured as indicated in this figure taken from *Bipolar*, where we happen to show the two cylinders having the same radius:

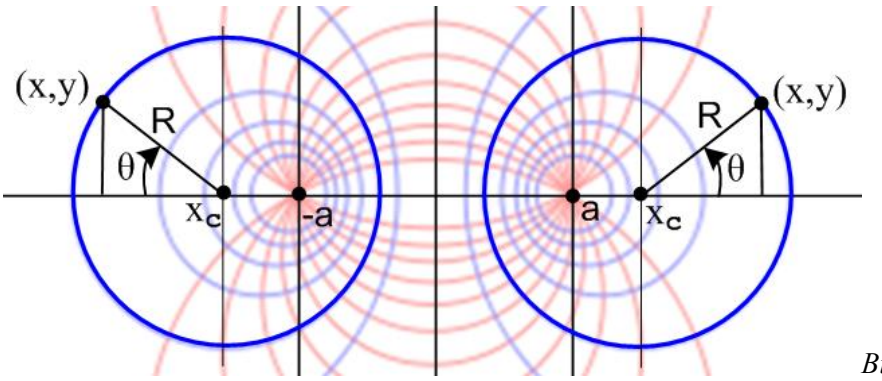

Bipolar (7.1) Fig 6.7

Notice that the two bipolar "focal points" are at x = ±a. In order to avoid confusion below, we shall always refer to this parameter in italics, *a*. The reason is that we shall be using non-italic a as the radius of the left cylinder, which in *Bipolar* is called R_1.

Comment: It is shown in *Bipolar* Section 10 (d) that the "center of charge" for the surface charge distribution n(θ) is in fact the focal point for each conductor.

Here is the more general picture where the cylinders have different radii. The right cylinder has bipolar coordinate $\xi_2 > 0$ and the left has $\xi_1 < 0$

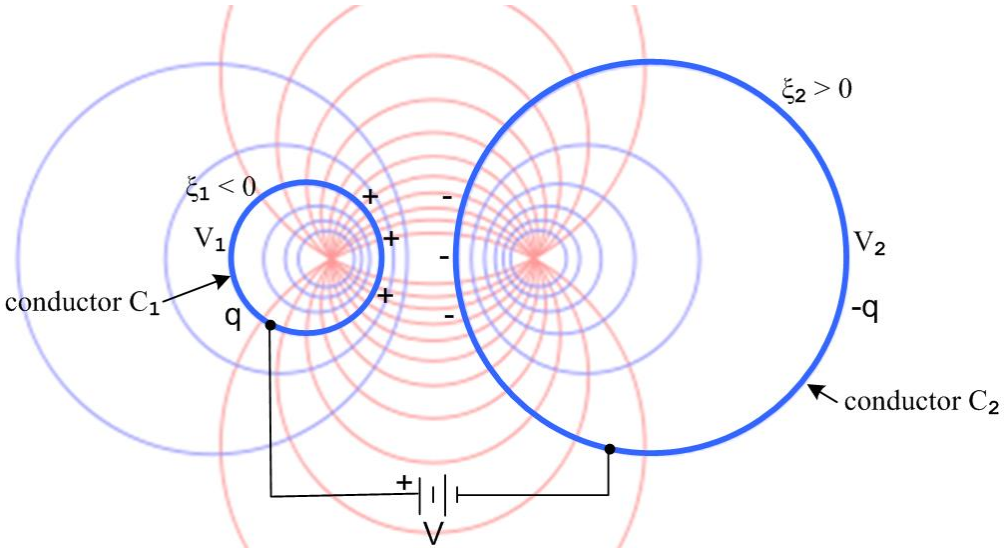

Bipolar (10.2) Fig 6.8

The angular surface charge densities on the conductors are found to be

$$n_1(\xi_1,\theta) = \frac{q}{2\pi}\,\frac{|\mathrm{sh}\xi_1|}{\mathrm{ch}\xi_1+\cos\theta}$$

$$n_2(\xi_2,\theta) = -\frac{q}{2\pi}\frac{|\mathrm{sh}\xi_2|}{\mathrm{ch}\xi_2+\cos\theta} \qquad \textit{Bipolar (10.28)} \qquad (6.5.1)$$

where

$$q = 2\pi\varepsilon\frac{V}{\xi_2-\xi_1} \qquad \textit{Bipolar (10.15)} \qquad (6.5.2)$$

and ε is of course for the dielectric between the conductors. Here q is the charge per unit length in z on the left conductor so has dimensions Cou/m. The surface charge density *n* is normalized so $\int n(\theta)d\theta = q$ so the dimensions of *n* are Cou/m. The true charge density is $n(\theta) = n(\theta)/a$ Cou/m^2.

The capacitance per unit length is then

$$C = q/V = 2\pi\varepsilon\frac{1}{\xi_2-\xi_1} \qquad \dim(\varepsilon) = \text{farad/m} \qquad \textit{Bipolar (10.16)} \qquad (6.5.3)$$

This is in agreement with (6.3.2) which says $K = 2(B_2-B_1) = 2(\xi_2-\xi_1)$ and (4.11.34) that $C = 4\pi\varepsilon/K$.

Notice that for fixed q the charge distribution on each conductor is independent of the ξ value of the other conductor. Thus, if the battery is disconnected, $n_1(\xi_1,\theta)$ does not change if ξ_2 is varied.

Using (D.1.5b) the moments of the surface charge distribution $n_1(\xi_1,\theta)$ are computed in *Bipolar* Appendix A and are found to be,

$$\eta_m \equiv N_m/N_0 = (-1)^m e^{-|m\xi_1|} . \qquad \textit{Bipolar (A.12)} \qquad (6.5.4)$$

Using (D.1.5a) one then finds,

$$n_1(\xi_1,\theta) = (q/2\pi)\left[1 + 2\sum_{m=1}^{\infty}(-1)^m e^{-m|\xi_1|}\cos(m\theta)\right] . \qquad \textit{Bipolar (A.13)} \qquad (6.5.5)$$

and in *Bipolar* Appendix A it is verified that this series sums to the expression in (6.5.1).

For small ξ_1 there are many significant partial waves in the sum. At θ = 0 the partial waves tend to cancel due to the alternating signs of the terms due to $(-1)^m$, whereas at θ = π the terms reinforce. As expected, the charge density peaks on the side of the conductor facing the other conductor. Here are plots of the charge distribution $n_1(\xi_1,\theta)$ (6.5.1) for various values of ξ_1 and for fixed q ($q/1\pi = 1$):

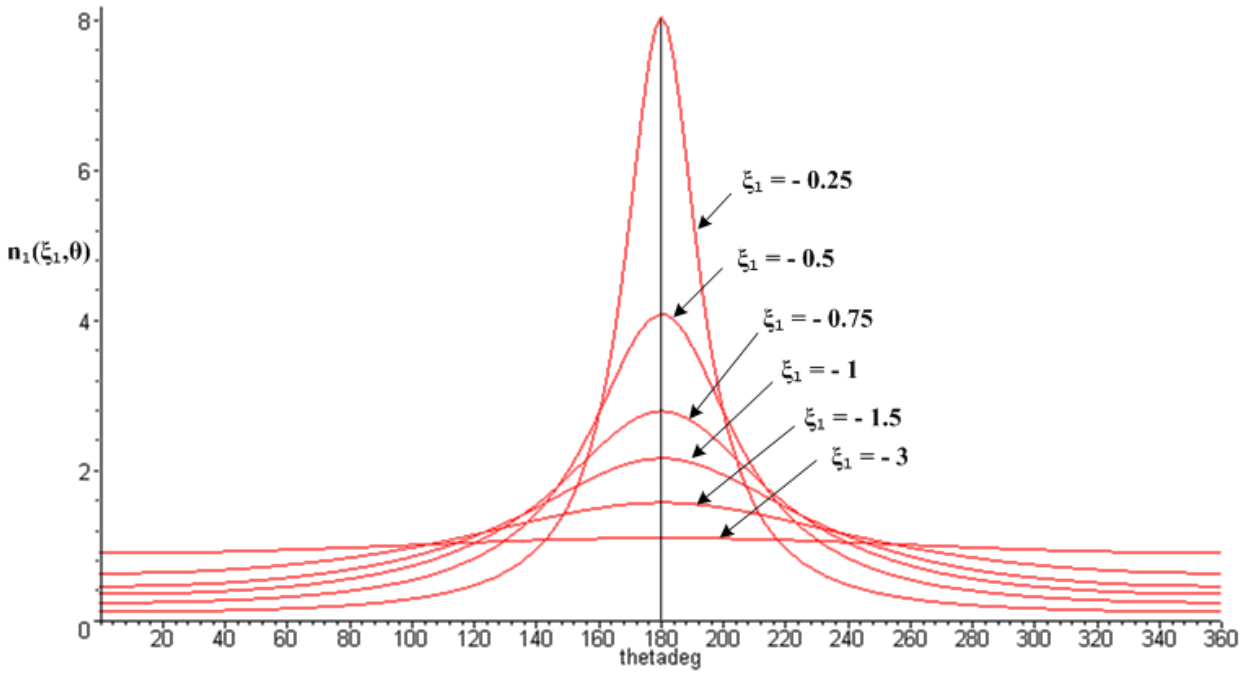

Bipolar (10.40) Fig 6.9

Here are some equations of interest, where the reader is reminded of the distinction between a and *a* noted below Fig 6.7 above :

$R_1 = a/|\mathrm{sh}\xi_1|$ // radius of left circle
$R_2 = a/|\mathrm{sh}\xi_2|$ // radius of right circle
$b = a(\coth\xi_2 - \coth\xi_1)$ // distance between center lines *Bipolar (11.3)* (6.5.6)

$a = (1/2b)\sqrt{b^2 - (R_2+R_1)^2}\sqrt{b^2 - (R_2-R_1)^2}$
$\xi_2 = \mathrm{sh}^{-1}(a/R_2)$
$\xi_1 = -\mathrm{sh}^{-1}(a/R_1)$. *Bipolar (11.10)* (6.5.7)

The first equation of the second set determines the bipolar focal distance *a* from the two cylinder radii R_1 and R_2 and the distance b between their center lines. For $R_1 = R_2 = a$ this says $a = (1/2)\sqrt{b^2-4a^2}$.

(b) The Proximity Effect

Appendix D computes the E fields inside a round wire of radius a in terms of the charge moments η_m . From (D.2.33) we have these partial wave components for E_z .

$E_z(r,m) = (1/4)\, I\, R_{dc}\, x_a\, \eta_m\, f_m$ where

$f_m \equiv \left[\frac{J_m(x)}{J_{m+1}(x_a)} - \frac{J_m(x)}{J_{m-1}(x_a)}\right]$ $x = \beta' r$ $x_a = \beta' a$ J_m = Bessel

$R_{dc} = \frac{1}{\sigma\pi a^2}$ = DC resistance of wire per unit length = ohms/m . (6.5.8)

Note that x, x_a and f_m are all dimensionless. From (D.2.2),

$$\beta'^2 \equiv \beta^2 - \beta_d^2 \qquad \textit{(D.2.2)}$$

where

$$\beta = e^{j3\pi/4}(\sqrt{2}/\delta) = (j-1)/\delta \qquad \text{wavenumber in conductor} \qquad \textit{(2.2.30)} \qquad (6.5.9)$$

$$\beta_d = (\omega/v_d) \ . \qquad \text{wavenumber in dielectric} \ . \qquad // \ v = \omega/k \qquad (6.5.10)$$

Below (D.2.2) we shown that $\beta' \approx \beta$ for any frequency $f << 10^{18}$ Hz, so we take

$$\beta' = \beta = e^{j3\pi/4}(\sqrt{2}/\delta) = (j-1)/\delta \ . \qquad (6.5.11)$$

Since $J_{-m}(x) = (-1)^m J_m(x)$ we find that

$$J_{-m}(x) = (-1)^m J_m(x) \qquad J_{-m+1} = (-1)^{m+1} J_{m-1} \qquad J_{-m-1} = (-1)^{m+1} J_{m+1}$$

so

$$f_{-m} = \left[\frac{J_{-m}(x)}{J_{-m+1}(x_a)} - \frac{J_{-m}(x)}{J_{-m-1}(x_a)}\right] = -\left[\frac{J_m(x)}{J_{m-1}(x_a)} - \frac{J_m(x)}{J_{m+1}(x_a)}\right] = f_m \ .$$

For the two cylinder problem we found above that $\eta_m = (-1)^m e^{-|m\xi_1|}$ so $\eta_{-m} = \eta_m$. To summarize:

$$f_{-m} = f_m$$
$$\eta_{-m} = \eta_m \ . \qquad (6.5.12)$$

The field $E_z(r,\theta)$ is then given by (D.1.3a),

$$E_z(r,\theta) = \sum_{m=-\infty}^{\infty} E_z(r,m)\, e^{jm\theta} = (1/4)\, I\, R_{dc}\, x_a \sum_{m=-\infty}^{\infty} \eta_m f_m e^{jm\theta}$$

$$= I R_{dc} (x_a/4) \left[f_0 + \Sigma_{m=1}^{\infty} \eta_m f_m e^{jm\theta} + \Sigma_{m=-\infty}^{-1} \eta_m f_m e^{jm\theta} \right]$$

$$= I R_{dc} (x_a/4) \left[f_0 + \Sigma_{m=1}^{\infty} \eta_m f_m e^{jm\theta} + \Sigma_{m=1}^{\infty} \eta_{-m} f_{-m} e^{-jm\theta} \right]$$

$$= I R_{dc} (x_a/4) \left[f_0 + 2 \Sigma_{m=1}^{\infty} \eta_m f_m \cos(m\theta) \right]$$

$$= I R_{dc} (\beta a/4) \left[f_0(r) + 2 \Sigma_{m=1}^{\infty} (-1)^m e^{-m|\xi_1|} f_m(r) \cos(m\theta) \right] \qquad (6.5.13)$$

and then using $J_{DC} = (I/\pi a^2)$,

$$J_z(r,\theta) = \sigma E_z(r,\theta) = (I/\pi a^2)(\beta a/4) \left[f_0(r) + 2 \Sigma_{m=1}^{\infty} (-1)^m e^{-m|\xi_1|} f_m(r) \cos(m\theta) \right] \text{ where}$$

$$f_m \equiv \left[\frac{J_m(x)}{J_{m+1}(x_a)} - \frac{J_m(x)}{J_{m-1}(x_a)}\right] \qquad x = \beta r \qquad x_a = \beta a \qquad \beta = e^{j3\pi/4}(\sqrt{2}/\delta) \ . \qquad (6.5.14)$$

This is the asymmetric current density in the left round conductor (the one with $\xi_1 < 0$) and just the fact that it is not constant shows that we have a **proximity effect** as illustrated in Fig 6.6 above.

(c) Plots of the Proximity Effect

First, it is helpful to have a plot showing the conductors for various values of ξ. so one can get a feel for how "fat" the cylinders are relative to their separation distance (same as Fig 6.2),

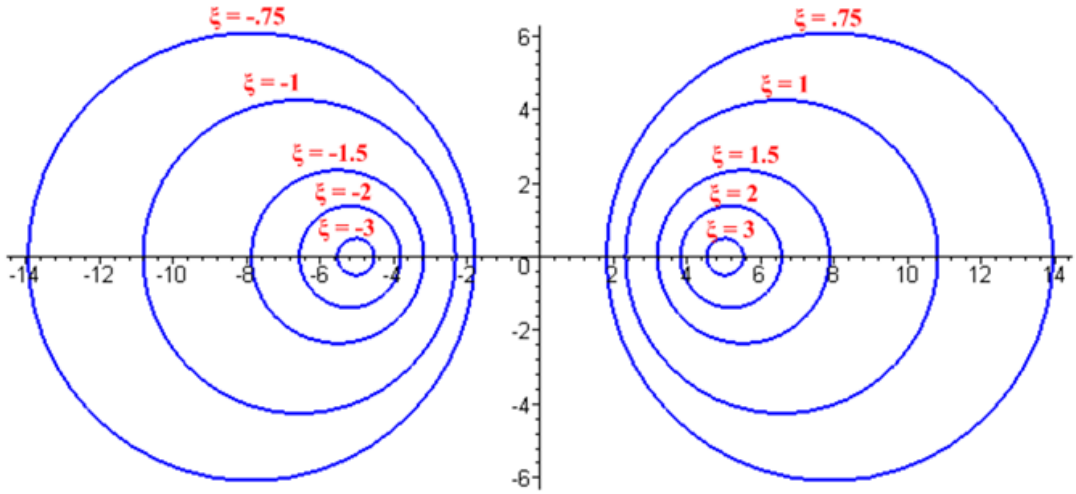

Bipolar (2.5) Fig 6.10

From (6.5.14), using $J_{DC} = (I/\pi a^2)$,

$$J_z(r,\theta) = J_{dc}\,(\beta a/4)\,[\ f_0(r) + 2\,\Sigma_{m=1}^{\infty}\,(-1)^m\,e^{-m|\xi_1|}\,f_m(r)\cos(m\theta)\ ] \quad . \qquad (6.5.15)$$

In Maple code we first enter all the expressions of interest,

```
restart; alias(J=BesselJ,I=I,j=sqrt(-1));
```

```
Jz := Jdc * (beta*a/4)*( f(0) + 2*Sum(eta(m)*f(m)*cos(m*theta),m=1..N) );
```

$$Jz := \frac{1}{4} Jdc\ \beta\ a \left(f(0) + 2 \left(\sum_{m=1}^{N} \eta(m)\, f(m) \cos(m\,\theta) \right) \right)$$

```
beta := exp(j*3*Pi/4) * sqrt(2) / delta;
```

$$\beta := \frac{\left(-\frac{1}{2}\sqrt{2} + \frac{1}{2} j \sqrt{2} \right) \sqrt{2}}{\delta}$$

```
f:= m ->J(m,x)/J(m+1,xa) -  J(m,x)/J(m-1,xa);
```

$$f := m \to \frac{J(m, x)}{J(m+1, xa)} - \frac{J(m, x)}{J(m-1, xa)}$$

```
eta := m -> (-1)^m*exp(-m*abs(xi1));
```

$$\eta := m \to (-1)^m\, \mathbf{e}^{(-m\,|\xi 1|)}$$

```
x := beta*r:   xa := beta*a:
```

Next, specific parameters are entered (xi1 = ξ_1)

```
N := 10:        # number of terms in sum
Jdc := 1:       # normalized DC current
xi1 := -1.00:   # label for left cylinder
a := 10:        # wire radius
delta := 1:     # skin depth
```

The first plot is of $|J_z(r,\theta)|$ where the axes are r and θ :

```
plot3d(abs(evalf((Jz))),r = 0..a,theta = 0..2*Pi, axes = boxed);
```

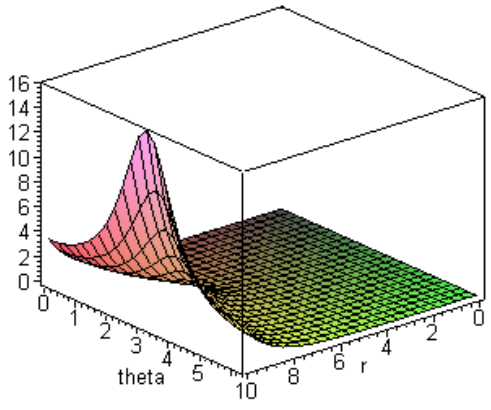

Fig 6.11

This shows the general peaking of $|J_z(r,\theta)|$ at θ = π, but the plot we really want to see is this:

```
r := sqrt(X^2+Y^2):
theta := arctan(Y,-X):    # note that X = -r*cos(theta) for left wire
plot3d(abs(evalf(Jz)),X = -a..a,Y = -sqrt(a^2-X^2)..sqrt(a^2-X^2), axes = boxed,
grid = [20,20]);
```

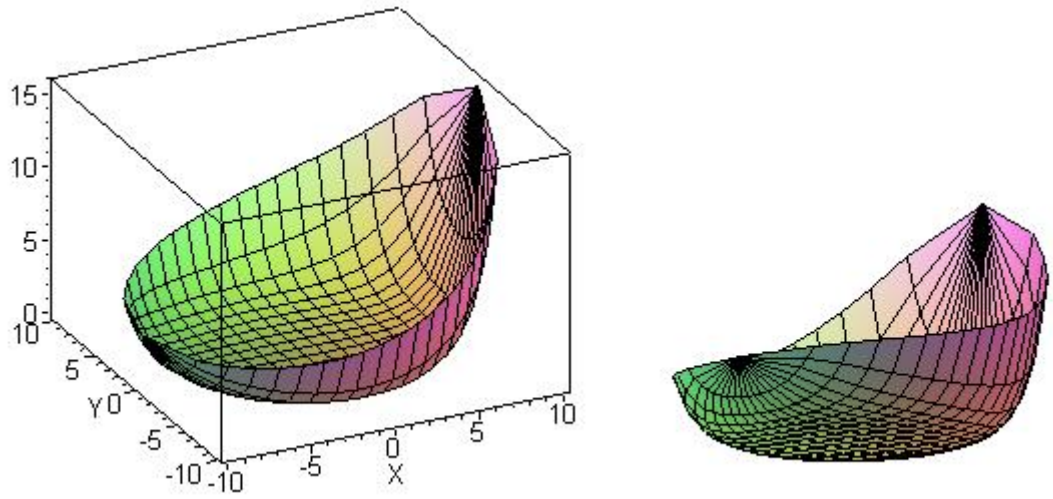

Fig 6.12

$|J_z|$ Distribution in left round wire for a = 10, δ = 1 and ξ_1 = - 1.00

Observations:

• Skin effect for $|J_z|$ appropriate to δ/a = 1/10 is seen in the cross section. The "bottom" of the plot is flat at value 0 and indicates no current in the central conductor region -- all current is in the sheath of thickness ≈ 1 just inside the wire radius a = 10.

• The distribution is strongly peaked on the side of the conductor facing the other conductor, and this is the proximity effect.

We now present a few such plots for different values of δ and ξ_1;

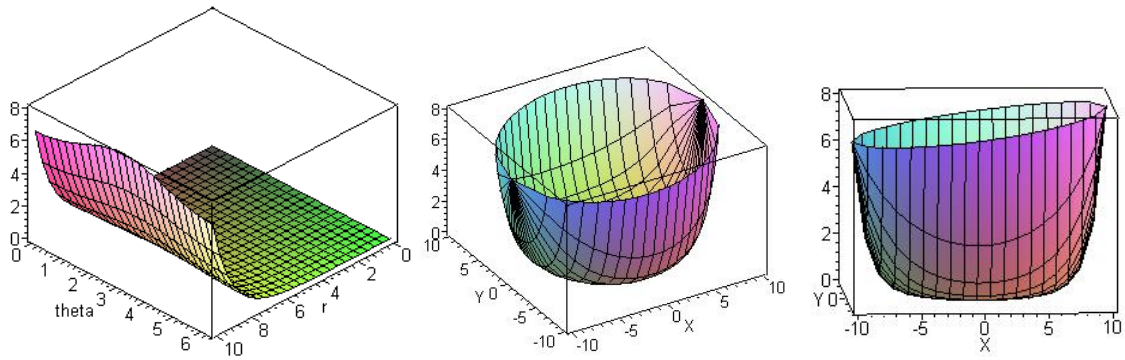

$|J_z|$ Distribution in left round wire for a = 10, δ = 1 and ξ_1 = - 3.00 Fig 6.13

Here, for two equal radius round wires of ξ_1= -3 and ξ_2= 3, the wires are "far apart" (see Fig 6.10 above). The proximity effect is still present as shown in the rightmost picture (larger at x = 10 than at x = -10), but the effect is small. On the other hand, the skin effect is still strongly in evidence, and again the entire current is in a sheath just inside r = a = 10 of thickness about δ = 1 unit.

Next:

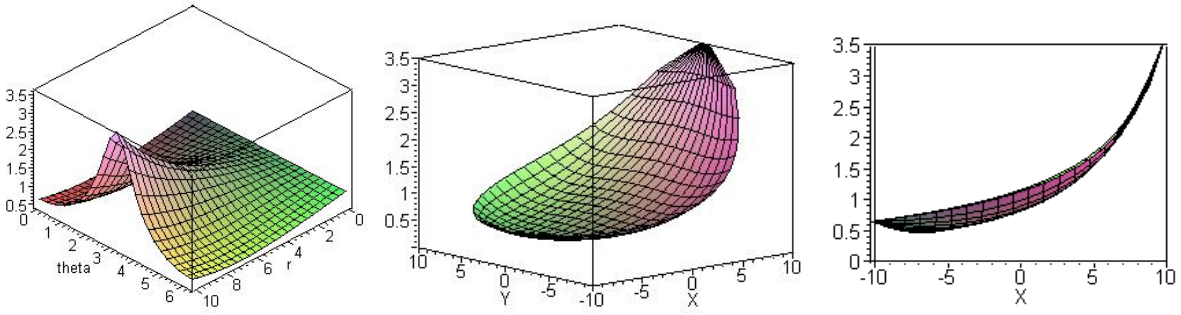

$|J_z|$ Distribution in left round wire for a = 10, δ = 5 and ξ_1 = - 1.00 Fig 6.14

In the central drawing we are looking into the bowl of the distribution from above. Since δ/a = 1/2 now, the skin effect is much less pronounced: J_z is no longer 0 in the central region as shown on the right. There is only a shallow "lip" around the bowl edge suggesting some skin effect. On the other hand, the proximity effect is still strong since for ξ_1 = -1 and ξ_2 = 1 the wires are fairly close together as shown in Fig 6.10. For such wires, using (6.5.6),

$$a/b = R_1/b = \frac{|\text{csch}\xi 1|}{\coth\xi_2 - \coth\xi_1} = \frac{|\text{csch}(-1)|}{\coth(1)-\coth(-1)} = \frac{\text{csch}(1)}{2\coth(1)} = \frac{1}{2\cosh(1)} = 0.324$$

$$\Longrightarrow \; b/a = 3.08 \quad \text{and} \quad b/(2a) = 1.54$$

so the ratio of wire center separation to wire diameter is about 1.5 (which agrees with ruler measurements made on Fig 6.10 above).

In the next plot, we have a = 10 and δ = 1, but now we plot the value of J_z at r = a going around the surface of the conductor for a set of different ξ_1 values:

```
r := a: N := 30:
plot([seq(abs(evalf(Jz)),xi1 = [-0.25,-0.5,-.75,-1,-1.5,-3])],theta =
0..2*Pi,color=red);
```

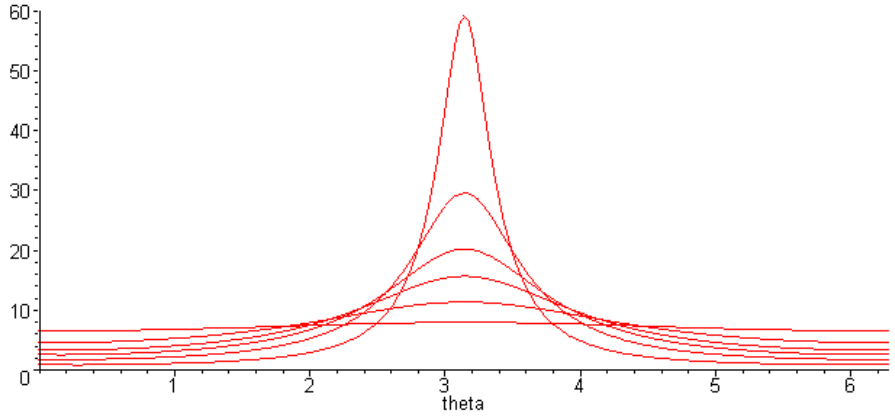

Fig 6.15

This plot of J_z bears a strong resemblance to the surface charge density plots shown above in Fig 6.9 for the same set of ξ_1 values. We show why this is so in the next two sections.

(d) The relationship between $J_z(a,\theta)$ and $n(\theta)$: the div E = 0 approach

Here, assuming the skin effect regime and making some wobbly assumptions, we obtain this relationship directly from the div **E** = 0 equation and the charge pumping boundary condition, just to provide some intuition about the linkage between J_z and $n(\theta)$. In the next section, we obtain the same result by taking the skin effect limit of (6.5.14) with no assumptions.

The charge pumping boundary condition of Appendix D says

$$E_r(r=a,\theta) = (j\omega/\sigma)\, n(\theta)\ . \qquad \textit{(D.2.24)} \qquad (6.5.16)$$

so the pattern of $n(\theta)$ is directly mapped to $E_r(r=a,\theta)$ at the surface. But we are interested in E_z since our current density of interest is $J_z = \sigma E_z$. The condition div **E** = 0 in cylindrical coordinates reads,

$$\partial_r\,(r\,E_r(r,\theta)) + \partial_\theta E_\theta(r,\theta) + r\,\partial_z E_z(r,\theta) = 0\ .$$

For r = a we know that $E_\theta(a,\theta) = 0$ from (3.7.1), so for r just below the surface we expect

$$\partial_r\,(r\,E_r(r,\theta)) + r\,\partial_z E_z(r,\theta) \approx 0 \qquad \text{// near r = a}$$

$$\partial_r\,(r\,E_r(r,\theta)) - j\beta_d\, r\,E_z(r,\theta) \approx 0 \qquad \text{// using } \partial_z \rightarrow -j\beta_d \text{, see (D.1.16)}$$

$$E_z(r,\theta) \approx (1/j\beta_d)\,(1/r)\,\partial_r\,(r\,E_r(r,\theta))\ . \qquad \text{// near r = a} \qquad (6.5.17)$$

For the symmetric-environment round wire, we know from (2.2.29) that

$$E_z(r) = E_z(a)\,\frac{J_0(\beta r)}{J_0(\beta a)}\ . \qquad (2.2.29)$$

If we blindly assume this same equation applies to $E_r(r,\theta)$ and $E_r(a,\theta)$, and if we take the large argument limits of the two Bessel functions using (2.3.3) and (2.3.6), we find that in the skin effect regime,

$$E_r(r,\theta) \approx E_r(a,\theta)\sqrt{\frac{a}{r}}\ \ e^{(r-a)/\delta}\ e^{j(r-a)/\delta} \qquad (6.5.18)$$

which we note has the same general form as the simple result (2.1.8) with x = a-r which is $e^{-x/\delta}\ e^{-jx/\delta}$ and is also consistent with (2.3.7) (for E_z) for magnitude. Then (6.5.17) says,

$$E_z(a,\theta) \;=\; (1/j\beta_d)\,E_r(a,\theta)[\,(1/r)\,\partial_r\,(r\sqrt{\frac{a}{r}}\ \ e^{(r-a)/\delta}\,e^{j(r-a)/\delta})\,]\,|^{r=a}$$

$$= (1/ja\ \beta_d)\,E_r(a,\theta)\,[1/2 + (1+j)a/\delta\,] \qquad (6.5.19)$$

where the derivative is done by Maple,

```
f := r*sqrt(a/r)*exp((r-a)/delta)*exp(j*(r-a)/delta);
```

$$f := r\sqrt{\frac{a}{r}}\,e^{\left(\frac{r-a}{\delta}\right)}\,e^{\left(\frac{j\,(r-a)}{\delta}\right)}$$

```
g := (1/r)*diff(f,r):
r := a;
```

$$r := a$$

```
g;
```

$$\frac{\frac{1}{2}+\frac{a}{\delta}+\frac{aj}{\delta}}{a}$$

Then using the boundary condition (6.5.16) we get

$$E_z(a,\theta) = \ (1/ja\ \beta_d)\,[(1+j)a/\delta\,]\,(j\omega/\sigma)\,n(\theta) \qquad (6.5.20)$$

where we have ignored Maple's 1/2 since in the skin effect limit a >> δ. Then finally,

$$J_z(a,\theta) = \ (1/ja\ \beta_d)\,[(1+j)a/\delta\,]\,(j\omega)\,n(\theta)\ = (1/a\ \beta_d)\,[(1+j)a/\delta\,]\,(\omega)\,n(\theta)$$

$$= \ (v_d/a)\,[(1+j)a/\delta\,]\,n(\theta) \qquad v_d = \omega/\beta_d \qquad //\ \sec^{-1}\ \text{Cou/m}^2\ = \text{amp/m}^2$$

$$= (\,v_d/a)\,[\,(1+j)a/\delta\,]\,(1/a)\,n(\theta) \qquad (6.5.21)$$

and this shows why $J_z(a,\theta)$ has the same angular shape as $n(\theta) = n(\theta)/a$!

(e) The relationship between $J_z(a,\theta)$ and $n(\theta)$ as a limit of (6.5.14)

Fact 1: In the skin effect limit, $f_m = -2j$ for $r = a$, (6.5.22)

Proof: From (6.5.8) with $r = a$ we find that

$$f_m \equiv \left[\frac{J_m(x_a)}{J_{m+1}(x_a)} - \frac{J_m(x_a)}{J_{m-1}(x_a)}\right] \tag{6.5.23}$$

In Chapter 2 we had these equations needed to take the asymptotic limit of J_m

$$J_m(e^{j3\pi/4}z) = M_m(z)\, e^{j\theta_m(z)}. \tag{2.3.3}$$

$$M_m(z) \approx \frac{\exp(z/\sqrt{2})}{\sqrt{2\pi z}}\left[1 - \frac{m-1}{8\sqrt{2}\,z} + O(1/z^2)\right]$$

$$\theta_m(z) \approx (z/\sqrt{2}) + (\pi/2)[m - 1/4] + \frac{m-1}{8\sqrt{2}\,z} + O(1/z^2). \tag{2.3.5}$$

Looking at the first term in (6.5.23) we get, writing $x = e^{j3\pi/4}z$,

$$\frac{J_m(x_a)}{J_{m+1}(x_a)} = \frac{M_m(z_a)}{M_{m+1}(z_a)}\, e^{j[\theta_m(za) - \theta_{m+1}(za)]} \approx e^{j[\theta_m(za) - \theta_{m+1}(za)]}$$

$$= \text{expj}\,[\{(z_a/\sqrt{2}) + (\pi/2)[m - 1/4]\} - \{(z_a/\sqrt{2}) + (\pi/2)[m+1 - 1/4]\}$$

$$= \text{expj}\,[\{+(\pi/2)\,0\} - \{+(\pi/2)\,[1]\}] = \text{expj}\,[\{-\pi/2\}] = -j \tag{6.5.24}$$

Restating this algebra for the ratio in the second term in (6.5.23) gives +j, but then the minus sign between the two terms changes this to -j, so the result is -2j as claimed. QED

Trust but verify: Here is an evaluation of f_m for $a = 50$, $\delta = 1$ and $m = 3$:

```
f(m);
```

$$\frac{J\left(3, 50\left(-\frac{1}{2}\sqrt{2} + \frac{1}{2}j\sqrt{2}\right)\sqrt{2}\right)}{J\left(4, 50\left(-\frac{1}{2}\sqrt{2} + \frac{1}{2}j\sqrt{2}\right)\sqrt{2}\right)} - \frac{J\left(3, 50\left(-\frac{1}{2}\sqrt{2} + \frac{1}{2}j\sqrt{2}\right)\sqrt{2}\right)}{J\left(2, 50\left(-\frac{1}{2}\sqrt{2} + \frac{1}{2}j\sqrt{2}\right)\sqrt{2}\right)}$$

```
evalf(%);
```

$$-.01196954158 - 2.009981266\,j$$

Recalling now (6.5.14),

$$J_z(r,\theta) = (I/\pi a^2)(\beta a/4)\left[f_0(r) + 2\sum_{m=1}^{\infty}(-1)^m e^{-m|\xi_1|} f_m(r)\cos(m\theta)\right] \tag{6.5.14}$$

we immediately obtain this skin effect limit,

$$J_z(r,\theta) = (-2j)\,(I/\pi a^2)(\beta a/4)\,[\;1 + 2\,\Sigma_{m=1}^{\infty}\,(-1)^m\,e^{-m|\xi_1|}\cos(m\theta)\;]\;. \qquad (6.5.25)$$

But the object in square brackets also appears in (6.5.5),

$$n_1(\xi_1,\theta) = (q/2\pi)[\;1 + 2\sum_{m=1}^{\infty}(-1)^m\,e^{-m|\xi_1|}\cos(m\theta)\;]\;. \qquad \textit{Bipolar (A.13)} \qquad \textit{(6.5.5)}$$

allowing us to write

$$J_z(a,\theta) = (-2j)\,(I/\pi a^2)(\beta a/4)\,(2\pi/q)\,n_1(\xi_1,\theta)\quad . \qquad (6.5.26)$$

Before continuing with details, we see at once that $J_z(a,\theta)$ has the same angular distribution as the surface charge density $n_1(\xi_1,\theta)$. Now recall that

$$I = q\,v_d \qquad \textit{(4.11.19a)}$$

$$\beta = e^{j3\pi/4}\,(\sqrt{2}\,/\delta) \qquad \textit{(6.5.9)}$$

where v_d is light speed in the transmission line dielectric. Then we find,

$$\begin{aligned} J_z(a,\theta) &= (-2j)\,(I/\pi a^2)(\beta a/4)\,(2\pi/q)\,n_1(\xi_1,\theta) \\ &= (-j)\,(I/a^2)(\beta a)\,(1/q)\,n_1(\xi_1,\theta) = (-j)\,(v_d/a^2)(\beta a)\,n_1(\xi_1,\theta) \\ &= (-j)\,(v_d/a)([\,e^{j3\pi/4}\,(\sqrt{2}\,/\delta)]a)\,(1/a)\,n_1(\xi_1,\theta) \\ &= e^{-j2\pi/4}\,e^{j3\pi/4}\,(v_d/a)\,\sqrt{2}\;(a/\delta)\,(1/a)\,n_1(\xi_1,\theta) \\ &= e^{+j2\pi/4}\sqrt{2}\;(v_d/a)\,(a/\delta)\,(1/a)\,n_1(\xi_1,\theta) \\ &= (1+j)\,(v_d/a)\,(a/\delta)\,(1/a)\,n_1(\xi_1,\theta) \\ &= (v_d/a)\,(1+j)\,(a/\delta)\,(1/a)\,n_1(\xi_1,\theta) \qquad (6.5.27) \end{aligned}$$

which agrees with the result (6.5.21) of the previous section. This seems to justify the assumptions made in the derivation of that result. Both derivations rely on the charge pumping boundary condition (D.2.24).

(f) The Proximity Effect At Low Frequencies

In various places in the above analysis, it was assumed that ω is high enough to put the transmission line in either the strong or extreme skin effect regime of (3.7.3) which roughly means $\delta < a/10$. In order to base the analysis on "the capacitor problem" as we have done (the electro-quasi-static model), we had to avoid the low frequency range which, expressed in terms of skin depth δ, is roughly $a/10 < \delta < \infty$. Only

then could we be assured that φ = constant *and* A_z = constant on the conductor surfaces as declared in (3.7.4) and (3.7.20), and only then are the transmission line equations and parameter evaluations of Chapter 4 valid. Our analysis of the proximity effect presented above inherits all these assumptions (in addition to the requirement of being in the transmission line limit so λ >> a).

As described in the text section below (3.7.21), we might blindly assume that our transmission line theory is "ballpark valid" in the low frequency range, and then the proximity effect calculation as given above would also apply approximately. For example, if we use our program above with a = 10 and δ = 10, which is deep into the low frequency range, the plots look like this:

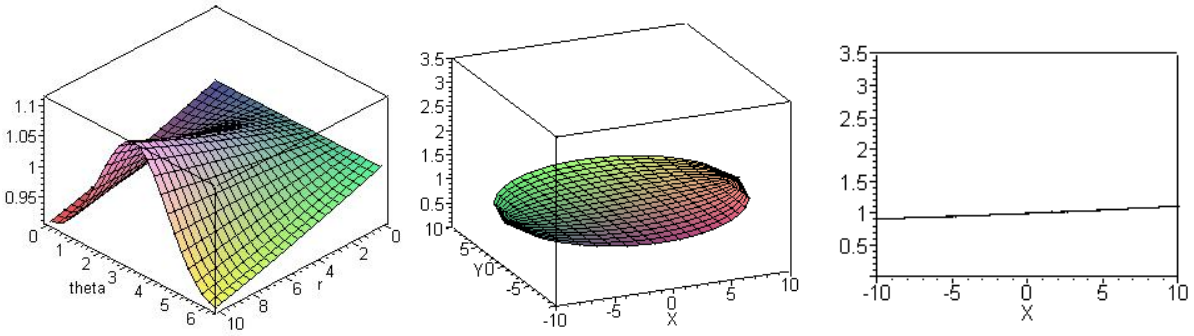

$|J_z|$ Distribution in left round wire for a = 10, δ = 20 and ξ_1 = - 3.00 Fig 6.16

The current distribution $|J_z|$ shown on the right is a flat disc which is almost horizontal but still has a very slight proximity effect visible in the right image. Since ξ_1 = -3 in this example, the conductors are "far apart", and we certainly expect intuitively to see a nearly flat $|J_z|$ distribution as we would see at DC (ω= 0, since no eddy currents).

However, if we instead use ξ_1 = -1.00, the program gives a strong proximity effect even if we lower the frequency way down to δ = 200:

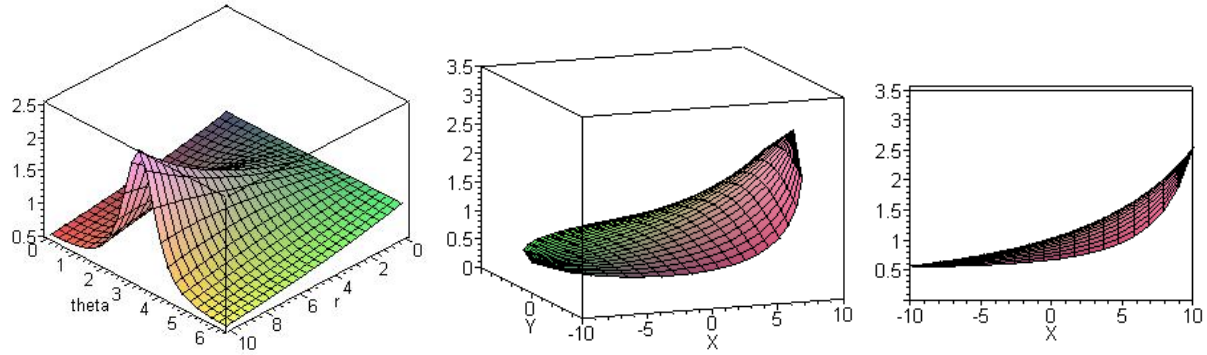

$|J_z|$ Distribution in left round wire for a = 10, δ = 200 and ξ_1 = - 1.00 Fig 6.17

Even at a very low frequency, the strongly peaked capacitor's n(θ) is maintained and "gets into" the $|J_z|$ distribution. This result seems incorrect and for such an example, our model blindly stretched to low ω seems to be giving a wrong result.

However, there is one sort of escape hatch to avoid this paradoxical limit as $\omega \rightarrow 0$. In the eddy current analysis of Section P.8, the two parallel cylinders considered there carry current I and -I. But our proximity effect described above is for a properly terminated active transmission line, not two wires that are shorted together at one end by an 8 ohm loudspeaker. A properly terminated transmission line, which we equate with the infinite transmission line this document addresses, must be terminated by Z_0. If we naively apply our theory as if it were valid at very low ω, we have

$$Z_0 \equiv V/I = \sqrt{\frac{\mathbf{z}}{\mathbf{y}}} = \sqrt{\frac{R + j\omega L}{G + j\omega C}} \quad . \qquad (4.11.16)$$

At very low ω, there is no dielectric displacement current and for "air" we can assume G = 0 (no conduction across the dielectric). Thus, in the limit $\omega \rightarrow 0$ we find that $Z_0 = \infty$. If we drive this transmission line with V = 10 volts at f = 0.1Hz, we find that I = 0 and there is no current at all, so that fact that it is asymmetric is not relevant.

Nevertheless, our suspicion is that the entire theory is only "ballpark accurate" at low ω, and therefore we have no trustworthy conclusions regarding the proximity effect at low frequencies.